7

THREE-DIMENSIONAL KINEMATICS AND KINETICS

7.0 INTRODUCTION

Over the past 20 years, there have been major commercial developments in three-dimensional (3D) hardware and software. Chapter 3 included descriptions of some of the 3D imaging systems that have been introduced. The majority of the systems are television-based, with multiple-camera arrangements requiring passive reflective markers, while other systems use active infrared emitting diodes (IRED) markers and infrared sensors. Regardless of the system used, the output of the data collection stage is a file of x, y, z coordinates of each of the markers at each sample point in time. These coordinates are in the global reference system (GRS) that is fixed in the laboratory or data collection space. The purpose of this chapter is to go through the steps where these coordinate data are transformed into the anatomical axes of the body segments so that a kinetic analysis can be done in a similar manner, as has been detailed for two-dimensional (2D) analyses in Chapters 3, 5, and 6.

7.1 AXES SYSTEMS

There are several axes reference systems that must be introduced in addition to the GRS already introduced. The markers that are placed on each segment provide a marker axis system that is a local reference system (LRS) for each individual segment. A second LRS is the axis system that defines the principal axis of each segment. Because skeletal landmarks are used to define these axes, this system is referred to as the anatomical axis system.

 Biomechanics and Motor Control of Human Movement, Fourth Edition David A. Winter
 ISBN: 978-0-470-39818-0

7.1.1 Global Reference System

For purposes of convenience, we will be consistent in our axis directions for the GRS: X is the forward/backward direction, Y is the vertical (gravitational) axis, and Z is the left/right (medial/lateral) axis. Thus, the XZ plane is the horizontal plane and, by definition, is orthogonal to the vertical axis. The directions of these GRS axes are the same as those of the axes in the force plate. To ensure that this is so, a spatial calibration system (a rigid cubic frame or a rigid 3D mechanical axis) is instrumented with markers and is placed on one of the force plates and aligned along the X and Z axes of the force platform. The position of each of the markers relative to the origin of the force plate is known and fed into the computer. If more than one force platform is used, the origin of each additional platform is recorded by an X and Z offset from the primary platform. An additional offset in the Y direction would be necessary if the additional platform were at a different height from the first (as would be necessary for a biomechanical analysis of stairway or ramp walking). Many laboratories have a fixed arrangement of cameras, so there is no need to recalibrate the GRS every day; such is the case in clinical gait laboratories. Such a system is illustrated in Chapter 3; see Figure 3.12. However, in many research situations, the cameras are rearranged to best capture the new movement and, therefore, require a new calibration of the GRS. Once the calibration is complete, the cameras cannot be moved, and care must be taken to ensure they are not accidentally displaced.

7.1.2 Local Reference Systems and Rotation of Axes

Within each segment, the anatomical axis system is set with its origin at the center of mass (COM) of the segment, and its principal y-axis usually along the long axis of the segment or, in the case of segments like the pelvis, along a line defined by skeletal landmarks such as PSIS and ASIS. The other local axis system is constructed on the segment by using a set of surface markers. A total of two transformations are necessary to get from the GRS to the marker axis system and from the marker to the anatomical axis system. Figure 7.1 shows how one of those rotations is done. The axis system x, y, z needs to be rotated into the system denoted by x''', y''', z'''. Many sequences of rotation are possible; here, we use the common Cardan sequence $x–y–z$. This means that we rotate about the x axis first, about the new y axis second, and about the new z axis last. The first rotation is θ_1 about the x axis to get x', y', z'. Because we have rotated about the x axis, x will not be changed and $x' = x$, while the y axis changes to $y'$and the z axis to z'. The second rotation is θ_2 about the new y' axis to get x'', y'', z''. Because this rotation has been about the y' axis, $y'' = y'$. The final rotation is θ_3 about the new z'' axis to get the desired x''', y''', z'''. Assuming that we have a point with coordinates x_0, y_0, z_0 in the original x, y, z axis system, that same

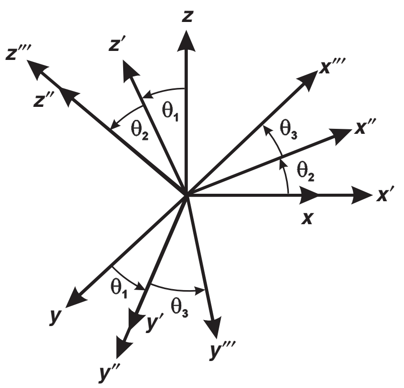

Figure 7.1 Cardan sequence of three rotations about the x, y, z axes. The first rotation, θ_1, about the x axis to get x', y', z'; the second rotation, θ_2, about the new y' axis to get x'', y'', z'', and the final rotation, θ_3, about the new z'' axis to get the desired x''', y''', z'''.

point will have coordinates x_1, y_1, z_1 in the x', y', z' axis system. Based on the rotation θ_1:

$$
\begin{aligned}
x_1 &= x_0 \\
y_1 &= y_0 \cos\theta_1 + z_0 \sin\theta_1 \\
z_1 &= -y_0 \sin\theta_1 + z_0 \cos\theta_1
\end{aligned}
$$

Using the shorthand notation $c_1 = \cos\theta_1$ and $s_1 = \sin\theta_1$, in matrix notation this may now be written as:

$$
\begin{bmatrix} x_1 \\ y_1 \\ z_1 \end{bmatrix} = \begin{bmatrix} 1 & 0 & 0 \\ 0 & c_1 & s_1 \\ 0 & -s_1 & c_1 \end{bmatrix} \begin{bmatrix} x_0 \\ y_0 \\ z_0 \end{bmatrix} = [\mathbf{\Phi}_1] \begin{bmatrix} x_0 \\ y_0 \\ z_0 \end{bmatrix} \tag{7.1}
$$

After the second rotation θ_2 about y', this point will have coordinates x_2, y_2, z_2 in the x'', y'', z'' axis system.

$$
\begin{bmatrix} x_2 \\ y_2 \\ z_2 \end{bmatrix} = \begin{bmatrix} c_2 & 0 & -s_2 \\ 0 & 1 & 0 \\ s_2 & 0 & c_2 \end{bmatrix} \begin{bmatrix} x_1 \\ y_1 \\ z_1 \end{bmatrix} = [\mathbf{\Phi}_2] \begin{bmatrix} x_1 \\ y_1 \\ z_1 \end{bmatrix} \tag{7.2}
$$

Finally, the third rotation θ_3 about z'' yields the coordinates x_3, y_3, z_3 in the x''', y''', z''' axis system.

$$
\begin{bmatrix} x_3 \\ y_3 \\ z_3 \end{bmatrix} = \begin{bmatrix} c_3 & s_3 & 0 \\ -s_3 & c_3 & 0 \\ 0 & 0 & 1 \end{bmatrix} \begin{bmatrix} x_2 \\ y_2 \\ z_2 \end{bmatrix} = [\mathbf{\Phi}_3] \begin{bmatrix} x_2 \\ y_2 \\ z_2 \end{bmatrix} \tag{7.3}
$$

Combining Equations (7.1), (7.2), and (7.3), we get:

$$\begin{bmatrix} x_3 \\ y_3 \\ z_3 \end{bmatrix} = [\boldsymbol{\Phi}_3]\,[\boldsymbol{\Phi}_2]\,[\boldsymbol{\Phi}_1] \begin{bmatrix} x_0 \\ y_0 \\ z_0 \end{bmatrix} \tag{7.4}$$

Note that the matrix multiplication as shown in Equation (7.4) is not commutative, which means that the order of the transformations must be such that $[\boldsymbol{\Phi}_1]$ is done first, $[\boldsymbol{\Phi}_2]$ second, and $[\boldsymbol{\Phi}_3]$ last. In other words, $[\boldsymbol{\Phi}_1][\boldsymbol{\Phi}_2] \neq [\boldsymbol{\Phi}_2][\boldsymbol{\Phi}_1]$. An expansion of Equation (7.4) yields:

$$\begin{bmatrix} x_3 \\ y_3 \\ z_3 \end{bmatrix} = \begin{bmatrix} c_2c_3 & s_3c_1 + s_1s_2c_3 & s_1s_3 - c_1s_2c_3 \\ -c_2s_3 & c_1c_3 - s_1s_2s_3 & s_1c_3 + c_1s_2s_3 \\ s_2 & -s_1c_2 & c_1c_2 \end{bmatrix} \begin{bmatrix} x_0 \\ y_0 \\ z_0 \end{bmatrix} \tag{7.5}$$

7.1.3 Other Possible Rotation Sequences

In theory, there are 12 possible correct rotation sequences; all were introduced by the Swiss mathematician, Leonhard Euler (1707–1783) . The list that follows gives all possible valid rotation sequences. The example explained previously is generally referred to as the Cardan system, which is commonly used in biomechanics, while the z–x–z rotation sequence, generally referred to as the Euler system, is commonly used in mechanical engineering.

$x - y' - x''$	$x - y' - z''$(Cardan)	$x - z' - x''$	$x - z' - y''$
$y - x' - y''$	$y - x' - z''$	$y - z' - x''$	$y - z' - y''$
$z - x' - y''$	$z - x' - z''$(Euler)	$z - y' - x''$	$z - y' - z''$

7.1.4 Dot and Cross Products

In 3D we are dealing almost exclusively with vectors and when vectors are multiplied we must compute the mathematical function called the *dot* or *cross product*. The dot product is also called the scalar product because the result is a scalar while the cross product is also called the vector product because the result is a vector. Dot product was first introduced in Section 6.08 in the calculation of the mechanical power associated with a force and velocity vector. Only the component of the force, F, and the velocity, V, that are parallel result in the power, $\mathrm{P} = \mathrm{F} \cdot \mathrm{V} = |\mathrm{F}||\mathrm{V}| \cos\theta$ where θ is the angle between F and V in the FV plane. In 3D the power $\mathrm{P} = \mathrm{F_x V_x} + \mathrm{F_y V_y} + \mathrm{F_z V_z}$.

Cross products are used to find the product of two vectors in one plane where the product is a vector nomal to that plane. Suppose we have vectors

$A = (A_x, A_y, A_z)$ and $B = (B_x, B_y, B_z)$ and the cross product is a vector C defined as $C = (A \times B)$. C is perpendicular to A and B in the direction defined by the right-hand rule and has a magnitude $= |A||B| \sin\theta$ where θ is the angle between A and B. The vector C is calculated by the expansion of the determinant where i, j, and k are unit vectors in the x, y, z axes:

$$C = A \times B = \begin{vmatrix} i & j & k \\ A_x & A_y & A_z \\ B_x & B_y & B_z \end{vmatrix}$$

$$\begin{aligned} C &= (AyBz - AzBy)i - (AxBz - AzBx)j + (AxBy - AyBx)k \\ &= iCx + jCy + kCz \end{aligned} \tag{7.6}$$

7.2 MARKER AND ANATOMICAL AXES SYSTEMS

The following description outlines the steps that are necessary to transform the x, y, z marker coordinates from the GRS to the anatomical axes of the segments of the person whose movement is being analyzed. Figure 7.2 presents the axis systems involved for a given segment whose COM is at c and whose axes $x{-}y{-}z$ are as shown. The GRS has axes $X{-}Y{-}Z$, and they are fixed for any given camera arrangement. The second axis system, $x_m{-}y_m{-}z_m$, is the marker axis system for each segment, and this can vary from laboratory to laboratory. Even within a given laboratory, each experiment could have a different arrangement of markers. For a correct 3D analysis, there must be at least three independent markers per body segment, and there must not be common markers between adjacent segments. The markers on each segment must not be collinear, which means they must not be in a straight line. They must form a plane in 3D space; as shown in Figure 7.2, the three tracking markers m_{T1}, m_{T2}, and m_{T3} define the tracking marker plane. This plane is assumed to contain the x_m and z_m axes such that all three markers are in the $+ve\, x_m$ and the $+ve\, z_m$ quadrant. One point on this marker plane is arbitrarily chosen as the origin of the marker axes system; here m_{T1} is chosen and is labeled m. The line from m_{T1} to m_{T3} defines the $+ve\, z_m$ axis; y_m is normal to the tracking plane, and x_m is orthogonal to the plane defined by $y_m{-}z_m$ to form a right-hand system.

The purpose of the anatomical calibration process is to find the relation between the marker axes, $x_m{-}y_m{-}z_m$, and the anatomical axes, $x{-}y{-}z$. This process requires the subject to assume a well-defined position; usually the anatomical position is used. At this time, extra calibration markers may be placed temporarily on the segment to define well-known anatomical points from which the segment's anatomical axes can be defined. For example, for

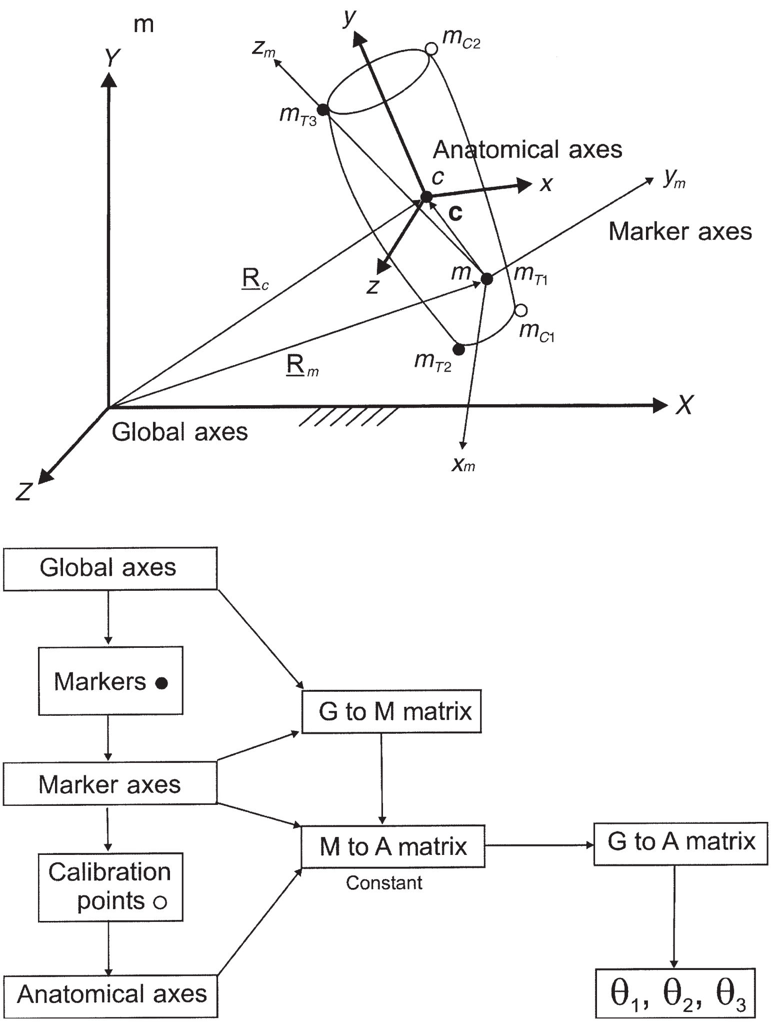

Figure 7.2 An anatomical segment showing the GRS, the marker axes, and anatomical axes. Three tracking markers, m_{T1}, m_{T2}, and m_{T3}, in conjunction with two calibration markers, m_{C1} and m_{C2}, define the constant [M to A] matrix. The three tracking markers in the GRS define the [G to M] matrix. The product of the variable [G to M] and the fixed [M to A] matrices gives the variable [G to A] matrix from which a new θ_1, θ_2, and θ_3 are defined for each frame.

the leg segment the three tracking markers could be placed on the head of the fibula (m_{T3}), on the lateral malleolus (m_{T2}), and at the midpoint on the anterior surface of the tibia (m_{T1}). During calibration, temporary markers, m_{C1} and m_{C2}, could be placed on the medial malleolus and the medial epicondyle of the tibia, respectively. With the subject standing still for about a second, the coordinates of the three tracking and the two calibration markers are recorded and averaged over the calibration time. The long axis of the leg segment (y axis) would then be defined as the line joining the midpoint between the lateral and medial malleolii (m_{T2} and m_{C1}) and the midpoint between the head of the fibula and the medial epicondyle of the tibia (m_{T3} and m_{C2}). These midpoints are the ankle and knee joints, respectively. The leg y axis and the line from m_{C1} to m_{T2} define a plane normal to which is the leg x axis. The direction of the leg z axis would be defined as a line normal to the leg $x-y$ plane such that the leg $x-y-z$ is a dextral system. The anatomical axes of the leg are now defined relative to the three tracking markers. The location of the center of mass of the leg would be a known distance along the y axis of the leg from the ankle joint; thus, the vector, **c**, from m, the origin of the tracking marker axis system, is also known. The two calibration markers are now removed and are no longer needed because the orientation of the axis system of the three tracking markers is now known and assumed to be fixed relative to the newly defined anatomical axes.

In clinical gait laboratories, it is impossible for many patients, such as cerebral palsy or stroke patients, to assume the anatomical position for even a short period of time. Thus, the clinical gait teams have developed a consistent marker arrangement combined with a number of specific anthropometric measures. These include such measures as ankle and knee diameters which, when combined with generic X-ray anthropometric measures, allow the team to input an algorithm so that offset displacements from the tracking markers to the joint centers are known. Patients are then asked to assume a static standing position with a number of temporary calibration markers similar to what has been described previously. In effect, the major single difference in the clinical laboratory is that calibration is performed on the patient in a comfortable standing position rather than the anatomical position. For the complete detailed steps in arriving at the joint kinetics in an operational clinical laboratory, the reader is referred to Davis et al. (1991) and Õunpuu et al. (1996).

In Figure 7.2, we see two matrix rotations. [G to M] is a 3×3 rotation matrix that rotates from the GRS to the tracking marker axes, $x_m - y_m - z_m$. This is a time-varying matrix because the tracking marker axes will be continuously changing relative to the GRS. [M to A] is a 3×3 matrix that rotates from the tracking marker axes to the anatomical axes. This matrix is assumed to be constant and results from the calibration protocol. The combination of these two rotation matrices gives us the [G to A] rotation matrix, which, when solved for a selected angle sequence, yields the three time-varying rotation angles, θ_1, θ_2, θ_3. With this final matrix, we can get the orientation of the anatomical axes directly from the tracking marker coordinates that are collected in the GRS.

However, from Figure 7.2, we are not yet finished. We also have to find a translational transformation to track the 3D coordinates of the segment COM, **c**, over time. The location of **c** is defined by the vector, $\mathbf{R}_c$, which is a vector sum of $\mathbf{R}_m + \mathbf{c}$. The vector $\mathbf{R}_m$ is the GRS coordinates of the tracking marker, m_{T1}, while $\mathbf{c}$ is a constant vector joining m to c, as defined earlier.

7.2.1 Example of a Kinematic Data Set

7.2.1.1 Calibration—Calculation of [Marker to Anatomical] Matrix. Let us now look at an example of numerical data to see how the various transformations are calculated. The leg segment in Figure 7.2 will be used as an example. Recall that there are three tracking markers on this segment plus two calibration markers whose coordinates were digitized during the calibration period when the subject stood steady in the anatomical position. In Figure 7.2, the subject would be facing the $+ve\ X$ direction, and the left leg was being analyzed. Table 7.1 gives the X, Y, and Z coordinates in the GRS, averaged over one second.

In this calibration position, the ankle $= (m_{T2} + m_{C1})/2$, $X_a = 2.815$, $Y_a = 10.16$, $Z_a = 22.685$.

The coordinates of the knee $= (m_{T3} + m_{C2})/2, X_k = 6.67, Y_k = 41.89$, $Z_k = 20.965$. The COM of the leg $= 0.567 \times \text{knee} + 0.433 \times \text{ankle}$, $X_c = 5.001, Y_c = 28.151, Z_c = 21.710$.

Now we have to locate the anatomical x, y, and z-axes. Let the line joining the ankle to the knee be the y axis, and the line joining the lateral malleolus to the medial malleolus be an interim z axis (because it is not exactly normal to the y axis but will be corrected later). These two axes now form a plane, and the x axis, by definition, is normal to the yz plane and, therefore, is the "cross product" of y and z, or $x_{an} = (y_{an} \times z_{an})$. Using the subscript "$an$" to indicate anatomical axes:

$$z_{an} = (m_{C1} - m_{T2}): \quad x_z = -0.21, \quad y_z = 0.21, \quad z_z = 7.67$$

$$y_{an} = (\text{knee} - \text{ankle}): \quad x_y = 3.855, \quad y_y = 31.73, \quad z_y = -1.72$$

$$x_{an} = (y_{an} \times z_{an}): \quad x_x = 243.575, \quad y_x = -29.207, \quad z_x = 7.126$$

One final correction must be done to our anatomical model. z_{an} is the line joining the medial to lateral malleolii and is approximately 90° from the long axis y_{an}. To ensure that all three anatomical axes are at right angles to

TABLE 7.1 Marker Coordinates during Standing Calibration

Marker	Location	X (cm)	Y (cm)	Z (cm)
m_{T1}	Midleg	9.39	30.02	21.90
m_{T2}	Lateral malleolus	2.92	10.10	18.85
m_{T3}	Fibular head	5.05	41.90	15.41
m_{C1}	Medial malleolus	2.71	10.22	26.52
m_{C2}	Medial condyle	8.29	41.88	26.52

each other, z_{an} must be corrected: $z_{an} = (x_{an} \times y_{an})$: $x_z = -176.872$, $y_z = 446.42, z_z = 7841.27$. Note that none of these vectors are unity length, and they are normally reported as a unit vector. For example, the length of x_{an} is 245.423 cm; thus, dividing each coordinate by the length of x_{an} yields a unity vector for $x_{an} : x_x = 0.9925, y_x = -0.1190, z_x = 0.290$. Similarly for y_{an} as a unit vector, $x_y = 0.1204, y_y = 0.9913, z_y = -0.0537$. Similarly as a unit vector, the corrected z_{an} is: $x_z = -0.0225$, $y_z = 0.0568$, $z_z = 0.9981$. We can now construct the leg anatomical-to-global matrix [LA to G] and it is:

$$\begin{bmatrix} 0.9925 & 0.1204 & -0.0225 \\ -0.1190 & 0.9913 & 0.0568 \\ 0.0290 & -0.0537 & 0.9981 \end{bmatrix}$$

Note that the diagonal values are almost = 1, indicating that the subject stood in the calibration position with his three anatomical axes almost perfectly lined up with the global axes. A more useful transformation matrix is the leg global-to-anatomical [LG to A], which is the transpose of [LA to G]:

$$\begin{bmatrix} 0.9925 & -0.1190 & 0.0290 \\ 0.1204 & 0.9913 & -0.0537 \\ -0.0225 & 0.0568 & 0.9981 \end{bmatrix}$$

These anatomical axes have their origins at the ankle joint. However, from our inverse dynamics, it is more convenient that the origin of the anatomical axes (see Figure 7.2) be located at the COM of the leg segment with coordinates 0, 0, 0. We must now establish the local coordinates of the ankle and knee joints and the three tracking markers relative to this new origin at the COM.

From the COM the ankle vector = (global ankle − global COM),

$$x_{al} = X_a - X_c = 2.815 - 5.001 = -2.186, y_{al} = Y_a - Y_c = 10.16 - 28.151$$
$$= -17.991, z_{al} = Z_a - Z_c = 22.685 - 21.710 = 0.975.$$

The anatomical ankle vector is the product of [LG to A][ankle vector]:

$$\begin{bmatrix} 0.9925 & -0.1190 & 0.0290 \\ 0.1204 & 0.9913 & -0.0537 \\ -0.0225 & 0.0568 & 0.9981 \end{bmatrix} \begin{bmatrix} -2.186 \\ -17.991 \\ 0.975 \end{bmatrix} = \begin{bmatrix} \approx 0 \\ -18.15 \\ \approx 0 \end{bmatrix}$$

This anatomical ankle vector lies along the line joining the ankle to knee and the ankle is 18.15 cm distal of the COM. The x and z components of this ankle vector are theoretically 0 but were calculated ≈0 because of the limited number of decimal points in our numbers. If we were to repeat this procedure for the anatomical knee vector and for the anatomical vectors of the three tracking markers m_{T1}, m_{T2} and m_{T3}, we would calculate the following:

$$\begin{array}{cccc} \text{Anatomical knee} & \text{Anatomical } m_{T1} & \text{Anatomical } m_{T2} & \text{Anatomical } m_{T3} \\ \text{vector} & \text{vector} & \text{vector} & \text{vector} \\ \begin{bmatrix} \approx 0 \\ 13.86 \\ \approx 0 \end{bmatrix} & \begin{bmatrix} 4.139 \\ 2.371 \\ 0.197 \end{bmatrix} & \begin{bmatrix} 0.000 \\ -17.991 \\ -3.833 \end{bmatrix} & \begin{bmatrix} -1.770 \\ 13.974 \\ -5.508 \end{bmatrix} \end{array}$$

We are now ready to calculate the constant marker-to-anatomical matrix ([M to A] in Figure 7.2). The three tracking markers form a plane in the GRS, and we can now define our maker axes in that plane. m_{T2} is chosen as the origin of the marker plane, and the line joining m_{T2} to m_{T3} is chosen to be the z axis, labeled z_m. The line joining m_{T2} to m_{T1} is a vector labeled **a** (an interim vector to allow us to calculate y_m and x_m). y_m is normal to the plane defined by z_m and A and x_m, is normal to the plane defined by y_m and z_m.

$$\begin{aligned} z_m &= \text{local } m_{T3} - \text{local } m_{T2} : [-1.770, 31.965, -1.675] \\ A \text{ vector} &= \text{local } m_{T1} - \text{local } m_{T2} : [4.139, 20.362, 4.030] \\ y_m &= (z_m \times A \text{ vector}) : [162.925, 0.200, -168.344] \\ x_m &= (y_m \times z_m) : [5380.78, 570.87, 5208.25] \end{aligned}$$

The normalized axis for this leg anatomical-to-marker matrix [LA to M] is:

$$\begin{bmatrix} 0.7164 & 0.0760 & 0.6935 \\ 0.6954 & 0.0008 & -0.7186 \\ -0.0552 & 0.9971 & -0.0522 \end{bmatrix}$$

The fixed leg marker-to-anatomical matrix [LM to A] is the transpose of [LA to M]:

$$\begin{bmatrix} 0.7164 & 0.6954 & -0.0552 \\ 0.0760 & 0.0008 & 0.9971 \\ 0.6935 & -0.7186 & -0.0522 \end{bmatrix}$$

7.2.1.2 Tracking Markers—Calculation of [Global to Marker] Matrix. We are now ready to calculate the [G to M] matrix in Figure 7.2. Table 7.2 lists representative GRS coordinates for the leg segment for three successive frames of walking taken during the swing phase. The procedure to calculate this [G to M] matrix is exactly the same as the latter part of the calculation of the [M to A] matrix. Consider the coordinates for frame 6:

$$\begin{aligned} \mathbf{z}_m &= (m_{T3} - m_{T2}) : [X_z = 24.34, Y_z = 19.99, Z_z = -3.64] \\ \mathbf{a} \text{ vector} &= (m_{T1} - m_{T2}) : [X_a = 18.86, Y_a = 9.15, Z_z = 4.09] \end{aligned}$$

TABLE 7.2 Tracking Markers during Walking

	m_{T1}			m_{T2}			m_{T3}		
Frame	X	Y	Z	X	Y	Z	X	Y	Z
5	20.65	33.87	35.95	1.30	25.74	32.14	26.52	44.43	28.10
6	25.46	34.47	35.95	6.60	25.32	31.86	30.94	45.31	28.22
7	30.18	34.97	35.94	11.98	24.64	31.60	35.08	46.10	28.36

$$y_m = (z_m \times \mathbf{a}) : [115.065, -168.201, -154.30]$$

$$x_m = (y_m \times z_m) : [3696.709, -3336.825, 6394.162]$$

The normalized axis for this leg [G to M] matrix for frame 6 is:

$$\begin{bmatrix} 0.4561 & -0.4117 & 0.7889 \\ 0.4501 & -0.6580 & -0.6037 \\ 0.7677 & 0.6305 & -0.1148 \end{bmatrix}$$

7.2.1.3 Calculation of [Global to Anatomical] Matrix. From Figure 7.2, the final step is to calculate the [G to A] matrix that is the product of the fixed [M to A] matrix and the variable [G to M] matrix; for frame 6 this product is:

$$\begin{bmatrix} 0.7164 & 0.6954 & -0.0552 \\ 0.0760 & 0.0008 & -0.9971 \\ 0.6935 & 0.7186 & -0.0522 \end{bmatrix} \begin{bmatrix} 0.4561 & -0.4117 & 0.7887 \\ 0.4501 & -.6580 & 0.6037 \\ 0.7677 & 0.6305 & -0.1148 \end{bmatrix}$$

$$= \begin{bmatrix} 0.5974 & -0.7873 & 0.1515 \\ 0.8000 & 0.5969 & -0.0550 \\ -0.0472 & 0.1544 & 0.9868 \end{bmatrix}$$

From Equation (7.5), this [G to A] matrix is equal to:

$$\begin{bmatrix} c_2c_3 & s_3c_1 + s_1s_2c_3 & s_1s_3 - c_1s_2c_3 \\ -c_2s_3 & c_1c_3 - s_1s_2s_3 & s_1c_3 + c_1s_2s_3 \\ s_2 & -s_1c_2 & c_1c_2 \end{bmatrix}$$

We now solve this matrix to get θ_1, θ_2, and θ_3. Equating the three terms in the bottom row: $s_2 = -0.0472$, $-s_1c_2 = 0.1544$, $c_1c_2 = 0.9868$. $\therefore \theta_2 = -2.71^\circ$ or 177.29°; assuming $\theta_2 = -2.71^\circ$, $c_2 = 0.99888$ or -0.99888, $c_1c_2 = 0.9868, \therefore c_1 = 0.9868/0.99888 = 0.9879$, and $\theta_1 = 8.92^\circ$ or -8.92°. $\therefore s_1 = 0.1550$ or -0.1550. We now validate that $\theta_1 = -8.92^\circ$ because $-s_1c_2 \approx 0.1544$. We now use the first two terms in the first column to calculate and validate $\theta_3 : c_2c_3 = 0.5974$, $-c_2s_3 = 0.8000$. $c_3 = 0.5974/0.99888$

$= 0.5981, \therefore \theta_3 = 53.27^\circ$ or -53.27°, and $s_3 = 0.8014$ or -0.8014. The only valid solution is $\theta_3 = -53.27^\circ$ because $-c_2 s_3 \approx 0.8000$. To summarize the results of these three rotations (see Figure 7.1), to bring the global axes in line with the anatomical axes requires an initial rotation about the global X axis of -8.92°. This will create new Y' and Z' axes and will be followed by a rotation of -2.71° about the Y' axis. This rotation creates new X'' and Z'' axes. The final rotation is the largest (because we are analyzing the leg segment during swing), and it is -53.27°, which creates the final X''', Y''', and Z''' axes. These final axes are the anatomical $x{-}y{-}z$ axes shown in Figure 7.2.

Finally, to get the COM of the segment, we must calculate **c** in GRS coordinates. We have **c** in the leg anatomical reference, and it is = – [Anatomical m_{T2} vector] = [0.0000, 17.991, 3.833]. In the GRS,

$$\begin{aligned}\mathbf{c} &= [\text{A to G}]\,[0.0000, 17.991, 3.833]\\ &= \begin{bmatrix} 0.5974 & 0.8000 & -0.0472 \\ -0.7873 & 0.5969 & 0.1544 \\ 0.1515 & -0.0550 & 0.9868 \end{bmatrix}\begin{bmatrix} 0.000 \\ 17.991 \\ 3.833 \end{bmatrix} = \begin{bmatrix} 14.212 \\ 11.346 \\ 2.793 \end{bmatrix}\end{aligned}$$

From Figure 7.2, the global vector $\mathbf{R}_c = \mathbf{R}_m + \mathbf{c} = [20.812, 36.646, 34.653]$.

As an exercise students can repeat these calculations for frames 5 and 7 with the answers:

$$\begin{aligned}&\text{Frame 5}: &&\theta_1 = -8.97^\circ, \theta_2 = -1.31^\circ, &&\theta_3 = -56.02^\circ,\\ & &&\mathbf{R}_c = [16.120, 36.325, 34.697] && \\ &\text{Frame 7}: &&\theta_1 = -8.56^\circ, \theta_2 = -4.08^\circ, &&\theta_3 = -49.89^\circ,\\ & &&\mathbf{R}_c = [25.429, 36.818, 34.623] &&\end{aligned}$$

7.3 DETERMINATION OF SEGMENT ANGULAR VELOCITIES AND ACCELERATIONS

Recall from Section 7.1.2 and Figure 7.2 that we had to determine three time-varying rotation angles, θ_1, θ_2, and θ_3, prior to transforming from the GRS to the anatomical axes. The first time derivative of these transformation angles yields the components of the segment angular velocities:

$$\boldsymbol{\omega} = d\theta_1/dt \cdot \mathbf{e}_x + d\theta_2/dt \cdot \mathbf{e}_{y'} + d\theta_3/dt \cdot \mathbf{e}_{z''} \tag{7.7a}$$

where $\mathbf{e}_x, \mathbf{e}_{y'}$ and $\mathbf{e}_{z''}$ denote the unit vectors of the three rotation axes x, y', and z'' shown in Figure 7.1. Consider an angular velocity, $\boldsymbol{\omega}'$, about axis x; here, $\boldsymbol{\omega}' = d\theta_1/dt \cdot \mathbf{e}_x$ and there is no rotation of θ_2 or θ_3. This angular velocity can be expressed as:

$$\boldsymbol{\omega}' = \begin{bmatrix} \dot{\theta}_1 \\ 0 \\ 0 \end{bmatrix}$$

The second angular velocity, $\boldsymbol{\omega}'' = d\theta_2/dt \cdot \mathbf{e}_{y'}$, plus the component of $\boldsymbol{\omega}'$ that is transformed by $[\boldsymbol{\Phi}_2]$ in Equation (7.2), can be expressed as:

$$\boldsymbol{\omega}'' = \begin{bmatrix} 0 \\ \dot{\theta}_2 \\ 0 \end{bmatrix} + \begin{bmatrix} c_2 & 0 & -s_2 \\ 0 & 1 & 0 \\ s_2 & 0 & c_2 \end{bmatrix} \begin{bmatrix} \dot{\theta}_1 \\ 0 \\ 0 \end{bmatrix} = \begin{bmatrix} 0 \\ \dot{\theta}_2 \\ 0 \end{bmatrix} + \begin{bmatrix} c_2\dot{\theta}_1 \\ 0 \\ s_2\dot{\theta}_1 \end{bmatrix} = \begin{bmatrix} c_2\dot{\theta}_1 \\ \dot{\theta}_2 \\ s_2\dot{\theta}_1 \end{bmatrix}$$

Similarly, the third angular velocity, $\boldsymbol{\omega}''' = d\theta_3/dt \cdot \mathbf{e}_{z''}$, plus the contribution from $\boldsymbol{\omega}''$ that is transformed by $[\boldsymbol{\Phi}_3]$ in Equation (7.3), gives us:

$$\begin{aligned} \boldsymbol{\omega}''' &= \begin{bmatrix} 0 \\ 0 \\ \dot{\theta}_3 \end{bmatrix} + \begin{bmatrix} c_3 & s_3 & 0 \\ -s_3 & c_3 & 0 \\ 0 & 0 & 1 \end{bmatrix} \begin{bmatrix} c_2\dot{\theta}_1 \\ 0 \\ s_2\dot{\theta}_1 \end{bmatrix} = \begin{bmatrix} 0 \\ 0 \\ \dot{\theta}_3 \end{bmatrix} + \begin{bmatrix} c_3c_2\dot{\theta}_1 + s_3\dot{\theta}_2 \\ -s_3c_2\dot{\theta}_1 + c_3\dot{\theta}_2 \\ s_2\dot{\theta}_1 \end{bmatrix} \\ &= \begin{bmatrix} c_3c_2\dot{\theta}_1 + s_3\dot{\theta}_2 \\ -s_3c_2\dot{\theta}_1 + c_3\dot{\theta}_2 \\ s_2\dot{\theta}_1 + \dot{\theta}_3 \end{bmatrix} \end{aligned}$$

Decomposing $\boldsymbol{\omega}'''$ into its three components along the three anatomical axes:

$$\boldsymbol{\omega} = \begin{bmatrix} \omega_x \\ \omega_y \\ \omega_z \end{bmatrix} = \begin{bmatrix} c_2c_3 & s_3 & 0 \\ -c_2s_3 & c_3 & 0 \\ s_2 & 0 & 1 \end{bmatrix} \begin{bmatrix} \dot{\theta}_1 \\ \dot{\theta}_2 \\ \dot{\theta}_3 \end{bmatrix} \tag{7.7b}$$

We can now calculate the three segment angular velocities, ω_x, ω_y, and ω_z, that are necessary to solve the 3D inverse dynamics equations developed in the next section. Recall that the time varying θ_1, θ_2, and θ_3 are calculated from Equation (7.5), and the time derivatives of these angles are individually calculated using the same finite difference technique used in two dimensions; see Equation (3.15). The three segment angular accelerations, α_x, α_y, and α_z, can now be calculated using either of the finite difference Equations (3.17) or (3.18c). We now have all the kinematic variables necessary for our 3D kinetic analyses.

7.4 KINETIC ANALYSIS OF REACTION FORCES AND MOMENTS

Having developed the transformation matrices from global to anatomical and from anatomical to global, we are now in a position to begin calculating the reaction forces and moments at each of the joints. Because the ground reaction forces are measured in the GRS and the moments of inertia are known in the anatomical axes, these previously determined transformation matrices are used extensively in the kinetic calculations. All joint reaction forces are initially calculated in the GRS, and all joint moments are calculated in the anatomical axes.

7.4.1 Newtonian Three-Dimensional Equations of Motion for a Segment

All reaction forces are calculated in the GRS and, because the gravitational forces and the segment COM accelerations are readily available in the GRS, it is convenient to calculate all segment joint reaction forces in the GRS. Students are referred to the 2D link-segment equations and free-body diagram equations in Section 5.1. Figure 7.3 is now presented to demonstrate the steps required to calculate kinetics for this segment. The only addition is the third dimension, z. We are given the three distal reaction forces either as measures from a force plate or from the analysis of the adjacent distal segment. It should be noted that the reaction forces and moments at the distal end are in the reverse direction from those at the proximal end, the same convention as was used in Section 5.1.

Step 1: Calculate the reaction forces at the proximal end of the segment in the GRS:

$$\Sigma F_X = ma_X \quad \text{or} \quad R_{XP} - R_{XD} = ma_X \tag{7.8a}$$

$$\Sigma F_Y = ma_Y \quad \text{or} \quad R_{YP} - R_{YD} - mg = ma_Y \tag{7.8b}$$

$$\Sigma F_Z = ma_Z \quad \text{or} \quad R_{ZP} - R_{ZD} = ma_Z \tag{7.8c}$$

where a_X, a_Y, a_Z are the segment COM accelerations in the X, Y, Z GRS directions and R_{XP}, R_{XD}, R_{YP}, R_{YD}, R_{ZP}, R_{ZD} are the proximal and distal reaction forces in the X, Y, and Z axes.

Step 2: Transform both proximal and distal reaction forces into the anatomical axes using the [G to A] matrix transformation based on θ_1, θ_2, and θ_3 [see Equation (7.5)]. We will now have the proximal and distal reaction forces in the anatomical axes x, y, z: R_{xp}, R_{xd}, R_{yp}, R_{yd}, R_{zp}, R_{zd}.

Step 3: Transform the distal moments from those previously calculated in the GRS using the [G to A] matrix to the anatomical axes, as before, based on θ_1, θ_2, and θ_3: M_{xd}, M_{yd}, M_{zd}. We now have all the variables necessary to calculate the proximal moments in the anatomical axes.

7.4.2 Euler's Three-Dimensional Equations of Motion for a Segment

The equations of motion for the 3D kinetic analyses are the Euler equations. Considerable simplification can be made in the rotational equations of motion if these equations are written with respect to the principal (anatomical) axes

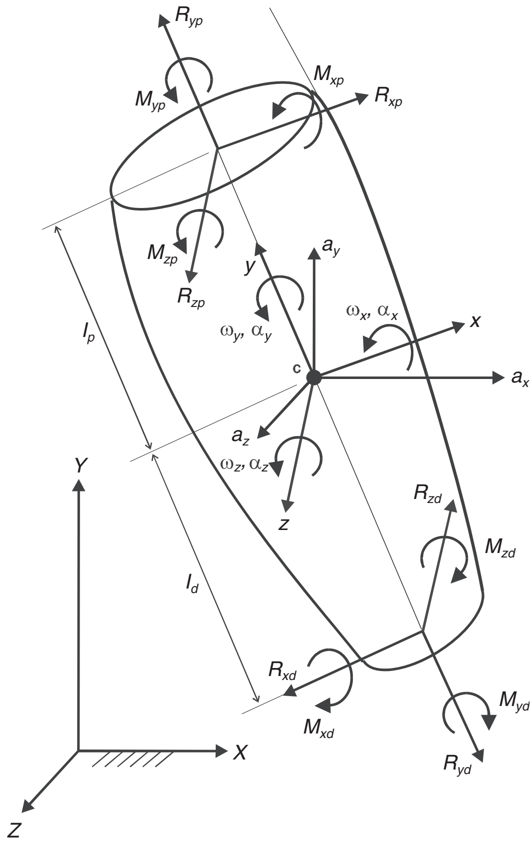

Figure 7.3 3D free-body diagram for solution of the inverse dynamics equations. Known are the distal reaction forces and moments, the COM linear accelerations, and the segment's angular velocities and accelerations. Using the kinetic Equations (7.8) and (7.9), we calculate the proximal reaction forces and moments.

of the segment with their origin at the COM of the segment. Thus, the $x-y-z$ axes of the segment in Figure 7.3 satisfy those conditions. The angular velocity of the segment in its coordinate system is ω. The rotational equations of motion are:

$$I_x\alpha_x + (I_z - I_y)\,\omega_y\omega_z = \Sigma M_x = R_{zd}l_d + R_{zp}l_p + M_{xp} - M_{xd} \quad (7.9a)$$

$$I_y\alpha_y + (I_x - I_z)\,\omega_x\omega_z = \Sigma M_y = M_{yp} - M_{yd} \quad (7.9b)$$

$$I_z\alpha_z + (I_y - I_x)\,\omega_x\omega_y = \Sigma M_z = -R_{xd}l_d - R_{xp}l_p + M_{zp} - M_{zd} \quad (7.9c)$$

where I_x, I_y, I_z = moments of inertia about $x-y-z$ axes

$\omega_x, \omega_y,$ and ω_z	= components of angular velocity $\boldsymbol{\omega}$ about $x-y-z$ axes
$\alpha_x, \alpha_y, \alpha_z$	= components of angular acceleration about $x-y-z$ axes
M_{xd}, M_{yd}, M_{zd}	= previously transformed distal moments (not shown in Figure 7.3) about $x-y-z$ axes
$R_{xd}, R_{xp}, R_{yd}, R_{yp}, R_{zd}, R_{zp}$	= previously transformed joint reaction forces about $x-y-z$ axes
l_p, l_d	= distances from COM to proximal and distal joints

The unknowns in these three equations are the three moments (M_{xp}, M_{yp} and M_{zp}) about the proximal x, y, z axes. Note that Equations (7.9) are in the same form as the 2D Equation (4.3) with the additional term $(I_1 - I_2)\ \omega_1\omega_2$ to account for the interaction of the angular velocities in the other two axes. Also note that the moments about the y axis (long axis of the segment) does not involve the proximal and distal reaction forces because these forces have zero moment arms about that axis.

7.4.3 Example of a Kinetic Data Set

The set of kinematic and kinetic data shown in Tables 7.3 and 7.4 is taken from stance phase of walking, and we will confine our analysis to the leg segment (see Figure 7.3). The following anthropometric measures apply: $m =$

TABLE 7.3 Ankle Reaction Forces (N) and Moments (N · m) in GRS

Frame	R_{XD}	R_{YD}	R_{ZD}	M_{XD}	M_{YD}	M_{ZD}
4	−86.55	−766.65	−13.81	10.16	6.74	−97.55
5	−102.71	−790.27	−12.12	11.94	4.65	−102.50
6	−119.04	−791.44	−12.03	14.29	2.11	−103.85
7	−134.33	−763.38	−10.26	16.13	−0.49	−101.32
8	−146.37	−704.00	−5.26	16.64	−2.88	−94.59

TABLE 7.4 Leg Angular Displacements (rad) and Velocities (rad/s)

Frame	θ_1	θ_2	θ_3	$\dot{\theta}_1$	$\dot{\theta}_2$	$\dot{\theta}_3$
4	−0.14246	−0.02646	−0.37248	−0.1752	0.2459	−2.358
5	−0.14512	−0.02362	−0.41396	−0.1607	0.0434	−2.641
6	−0.14781	−0.02501	−0.46053	−0.0911	−0.1048	−2.909
7	−0.14815	−0.02705	−0.51094	−0.1139	−0.0923	−3.209
8	−0.15161	−0.02809	−0.56749	−0.1109	0.2175	−3.472

3.22 kg, $I_x = 0.0138\,\text{kg}\cdot\text{m}^2$, $I_y = 0.0024\,\text{kg}\cdot\text{m}^2$, $I_z = 0.0138\,\text{kg}\cdot\text{m}^2$, $l_d = 13.86\,\text{cm}$, $l_p = 18.15\,\text{cm}$, frame rate = 60 Hz.

From the kinematic and kinetic measures presented in Tables 7.3 and 7.4, we complete the analysis of frame 6: $a_x = 7.029\,\text{m/s}^2, a_Y = 1.45\,\text{m/s}^2, a_Z = -.348\,\text{m/s}^2$. Refer to the three steps in Section 7.4.1.

Step 1

$$R_{XP} - R_{XD} = ma_X, \quad 0\ R_{XP} = -119.04 + 3.22 \times 7.029 = -96.41\ \text{N}$$

$$R_{YP} - R_{YD} - mg = ma_Y, \quad R_{YP} = -791.44 + 3.22 \times 9.814 + 3.22 \times 1.45 = -755.17\ \text{N}$$

$$R_{ZP} - R_{ZD} = ma_Z, \quad R_{ZP} = -12.03 + 3.22 \times (-.348) = -13.15\ \text{N}$$

Step 2

$$\theta_1 = -0.1478\,\text{rad} = -8.468^\circ, \theta_2 = -0.025\,\text{rad} = -1.432^\circ,$$
$$\theta_3 = -0.4605\,\text{rad} = -26.385^\circ$$

$$\begin{aligned} \cos\theta_1 &= 0.9891, & \sin\theta_1 &= -.1476 \\ \cos\theta_2 &= 0.9997, & \sin\theta_2 &= -0.025 \\ \cos\theta_3 &= 0.8958, & \sin\theta_3 &= -.4444 \end{aligned}$$

Substituting these values in the [G to A] matrix [Equation (7.5)], we get:

$$\begin{bmatrix} c_2c_3 & s_3c_1 + s_1s_2c_3 & s_1s_3 - c_1s_2c_3 \\ -c_2s_3 & c_1c_3 - s_1s_2s_3 & s_1c_3 + c_1s_2s_3 \\ s_2 & -s_1c_2 & c_1c_2 \end{bmatrix} = \begin{bmatrix} 0.8955 & -0.4363 & 0.0875 \\ 0.4443 & 0.8877 & -0.121 \\ -0.025 & 0.1473 & 0.9888 \end{bmatrix}$$

We can now transform the reaction forces from the global to the anatomical axes system:

$$\begin{bmatrix} R_{xd} \\ R_{yd} \\ R_{zd} \end{bmatrix} = \begin{bmatrix} 0.8955 & -0.4363 & 0.0875 \\ 0.4443 & 0.8877 & -0.121 \\ -0.025 & 0.1473 & 0.9888 \end{bmatrix} \begin{bmatrix} R_{XD} \\ R_{YD} \\ R_{ZD} \end{bmatrix}$$
$$= \begin{bmatrix} 0.8955 & -0.4363 & 0.0875 \\ 0.4443 & 0.8877 & -0.121 \\ -0.025 & 0.1473 & 0.9888 \end{bmatrix} \begin{bmatrix} -119.04 \\ -791.44 \\ -12.03 \end{bmatrix} = \begin{bmatrix} 237.65 \\ -754.00 \\ -125.50 \end{bmatrix}$$

$$\begin{bmatrix} R_{xp} \\ R_{yp} \\ R_{zp} \end{bmatrix} = \begin{bmatrix} 0.8955 & -0.4363 & 0.0875 \\ 0.4443 & 0.8877 & -0.121 \\ -0.025 & 0.1473 & 0.9888 \end{bmatrix} \begin{bmatrix} R_{XP} \\ R_{YP} \\ R_{ZP} \end{bmatrix}$$
$$= \begin{bmatrix} 0.8955 & -0.4363 & 0.0875 \\ 0.4443 & 0.8877 & -0.121 \\ -0.025 & 0.1473 & 0.9888 \end{bmatrix} \begin{bmatrix} -96.41 \\ -755.17 \\ -13.15 \end{bmatrix} = \begin{bmatrix} 241.99 \\ -711.61 \\ -121.83 \end{bmatrix}$$

Step 3: In a similar manner, we transform the ankle moments from the global to the anatomical axes system:

$$\begin{bmatrix} M_{xd} \\ M_{yd} \\ M_{zd} \end{bmatrix} = \begin{bmatrix} 0.8955 & -0.4363 & 0.0875 \\ 0.4443 & 0.8877 & -0.121 \\ -0.025 & 0.1473 & 0.9888 \end{bmatrix} \begin{bmatrix} M_{XD} \\ M_{YD} \\ M_{ZD} \end{bmatrix}$$

$$= \begin{bmatrix} 0.8955 & -0.4363 & 0.0875 \\ 0.4443 & 0.8877 & -0.121 \\ -0.025 & 0.1473 & 0.9888 \end{bmatrix} \begin{bmatrix} 14.29 \\ 2.11 \\ -103.85 \end{bmatrix} = \begin{bmatrix} 2.79 \\ 20.79 \\ -102.73 \end{bmatrix}$$

Using Equation (7.7*b*), we calculate the angular velocities and accelerations required for the solution of Euler's kinetic Equations (7.9). As previously calculated for frame 6, $c_2 = 0.9997$, $c_3 = 0.8958$, $s_2 = -0.025$, $s_3 = -0.4444$.

$$\begin{bmatrix} \omega_x \\ \omega_y \\ \omega_z \end{bmatrix} = \begin{bmatrix} c_2c_3 & s_3 & 0 \\ -c_2s_3 & c_3 & 0 \\ s_2 & 0 & 1 \end{bmatrix} \begin{bmatrix} \dot{\theta}_1 \\ \dot{\theta}_2 \\ \dot{\theta}_3 \end{bmatrix} = \begin{bmatrix} 0.8955 & -0.4444 & 0 \\ 0.4443 & 0.8958 & 0 \\ -0.025 & 0 & 1 \end{bmatrix} \begin{bmatrix} -0.0911 \\ -0.1048 \\ -2.909 \end{bmatrix}$$

$$= \begin{bmatrix} -0.0350 \\ -.1344 \\ -2.907 \end{bmatrix}$$

Similarly for frame 5,

$$\begin{bmatrix} \omega_x \\ \omega_y \\ \omega_z \end{bmatrix} = \begin{bmatrix} -0.1646 \\ -0.0249 \\ -2.637 \end{bmatrix}$$

and for frame 7,

$$\begin{bmatrix} \omega_x \\ \omega_y \\ \omega_z \end{bmatrix} = \begin{bmatrix} -0.0542 \\ -0.13621 \\ -3.206 \end{bmatrix}$$

We now calculate the angular accelerations of the segment where Δt is the sampling period:

$$\alpha_x(\text{fr.6}) = [\omega_x(\text{fr.7}) - \omega_x(\text{fr.5})]/2\Delta\text{t} = [-0.0542 - (-0.1646)]/0.03333$$
$$= 3.312\,\text{r/s}^2$$

$$\alpha_y(\text{fr.6}) = [\omega_y(\text{fr.7}) - \omega_y(\text{fr.5})]/2\Delta\text{t} = [-0.1362 - (-0.0249)]/0.03333$$
$$= -3.337\,\text{r/s}^2$$

$$\alpha_z(\text{fr.6}) = [\omega_z(\text{fr.7}) - \omega_z(\text{fr.5})]/2\Delta\text{t} = [-3.206 - (-2.637)]/0.03333$$
$$= -17.07\,\text{r/s}^2$$

We are now ready to solve Euler's Equations (7.9) for the proximal moments:

$$I_x\alpha_x + (I_z - I_y)\,\omega_y\omega_z = \Sigma M_x = R_{zd}l_d + R_{zp}l_p + M_{xp} - M_{xd}$$

$$M_{xp} = 2.79 + 121.83 \times 0.1815 + 125.5 \times 0.1386 + 0.0138 \times 3.312$$
$$+(0.0138 - 0.0024) \times 0.1344 \times 2.907 = 42.35\,\mathrm{N \cdot m}$$

$$I_y\alpha_y + (I_x - I_z)\,\omega_x\omega_z = \Sigma M_y = M_{yp} - M_{yd}$$

$$M_{yp} = 20.79 - 0.0024 \times 3.337 + (0.0138 - 0.0138) \times 0.035 \times 2.907$$
$$= 20.78\,\mathrm{N \cdot m}$$

$$I_z\alpha_z + (I_y - I_x)\,\omega_x\omega_y = \Sigma M_z = -R_{xd}l_d - R_{zp}l_p + M_{zp} - M_{zd}$$

$$M_{zp} = -102.73 + 241.99 \times 0.1815 + 237.65 \times 0.1386 - 0.0138$$
$$\times 17.07 + (0.0024 - 0.0138) \times 0.035 \times 0.1343 = -26.11\,\mathrm{N \cdot m}$$

The interpretation of these moments for the left knee is as follows as the subject bears weight during single support. M_{xp} is $+ve$; thus, it is a counterclockwise moment and hence an abductor moment acting at the knee to counter the large gravitational load of the upper body acting downward and medial of the support limb. M_{yp} is the axial moment acting along the long axis of the leg and reflects the action of the left hip internal rotators actively rotating the pelvis, upper body, and right limb in a forward direction to gain extra step length. M_{zp} is $-ve$, indicating a clockwise (flexor) knee moment in the sagittal plane that would assist in starting the knee to flex late in stance shortly before toe-off.

The next stage of the kinetic analysis is to transform these knee moments, M_{xp}, M_{yp}, and M_{zp} (which are in the leg anatomical axis system), to the global system so that the inverse dynamics analysis can continue for the thigh segment. This transformation is accomplished by the [A to G] matrix for the leg and yields a new set of distal moments, M_{XD}, M_{YD}, and M_{ZD}, for the thigh analysis.

As an exercise, students may wish to repeat the preceding calculations for frame 5 or 7. For frame 5: $a_X = 5.89\,\mathrm{m/s^2}$, $a_Y = 1.30\,\mathrm{m/s^2}$, $a_Z = -1.66\,\mathrm{m/s^2}$; for frame 7: $a_X = 9.60\,\mathrm{m/s^2}$, $a_Y = 1.94\,\mathrm{m/s^2}$, $a_Z = -.020\,\mathrm{m/s^2}$. For frame 5: $M_{xp} = 40.76\,\mathrm{N \cdot m}$, $M_{yp} = 21.61\,\mathrm{N \cdot m}$, $M_{zp} = -31.23\,\mathrm{N \cdot m}$; for frame 7: $M_{xp} = 41.85\,\mathrm{N \cdot m}$, $M_{yp} = 19.20\,\mathrm{N \cdot m}$, $M_{zp} = -19.80\,\mathrm{N \cdot m}$.

7.4.4 Joint Mechanical Powers

The joint mechanical power generated or absorbed at the distal and proximal joints, P_d and P_p, can now be calculated using Equation (5.5) for each of three moment components and their respective angular velocities:

$$P_d = M_{xd}\omega_{xd} + M_{yd}\omega_{yd} + M_{zd}\omega_{zd} \tag{7.10a}$$

$$P_p = M_{xp}\omega_{xp} + M_{yp}\omega_{yp} + M_{zp}\omega_{zp} \tag{7.10b}$$

where the moments are previously defined and ω_{xd}, ω_{yd}, ω_{zd}, ω_{xp}, ω_{yp}, and ω_{zp} are the joint angular velocities at the distal and proximal ends (not shown on Figure 7.3). The angular velocities are in rad/s, the moments are in N · m, and the powers are in W. If these products were $+ve$ the muscle group concerned would be generating energy, and if they were $-ve$, the muscle group would be absorbing energy.

7.4.5 Sample Moment and Power Curves

Figure 7.4 presents a set of intersubject averaged 3D joint moments at the ankle, knee, and hip during one walking stride (Eng and Winter, 1995). Heel contact (HC) is at 0% stride and toe-off (TO) is at 60%. Figure 7.5 shows the 3D power curves for these intersubject averages (Eng and Winter, 1995). The curves are normalized relative to body mass; the moments are reported in N · m/kg and the powers in W/kg. Convention plots extensor moments in the sagittal plane as positive; in the transverse plane, external rotation moments are positive, and in the frontal plane, evertor moments are positive. A detailed explanation of the specific function of each of these moments is beyond the scope of this text; however, a few comments will be made on the larger or functionally more important moments.

1. The largest moment during walking is seen at the ankle in the sagittal plane. Immediately at heel contact (HC), there is a small dorsiflexor moment to lower the foot to the ground; this is followed by a large increase in plantarflexor moment reaching a peak at about 50% of stride to cause the ankle to rapidly plantarflex and achieve an upward and forward "pushoff" of the lower limb as the subject starts swing at toe-off (TO) (see A2-S power generation burst in Figure 7.5).
2. The knee extensors are active at 8–25% of stride to control knee flexion as the limb accepts weight (K1-S absorption phase), then the moment reverses to a flexor pattern as a by-product of the gastrocnemic's contribution to the increasing ankle plantarflexor moment. Then, just before and after TO, a small knee extensor moment acts to limit the amount of knee flexion in late stance and early swing (K3-S absorption phase). The final burst of flexor activity just before HC is to decelerate the swinging leg prior to HC (K4-S absorption phase).
3. The hip pattern is characterized by an extensor moment for the first half of stance, followed by a flexor for the latter half. During the first half, the extensors stabilize the posture of the trunk by preventing it from

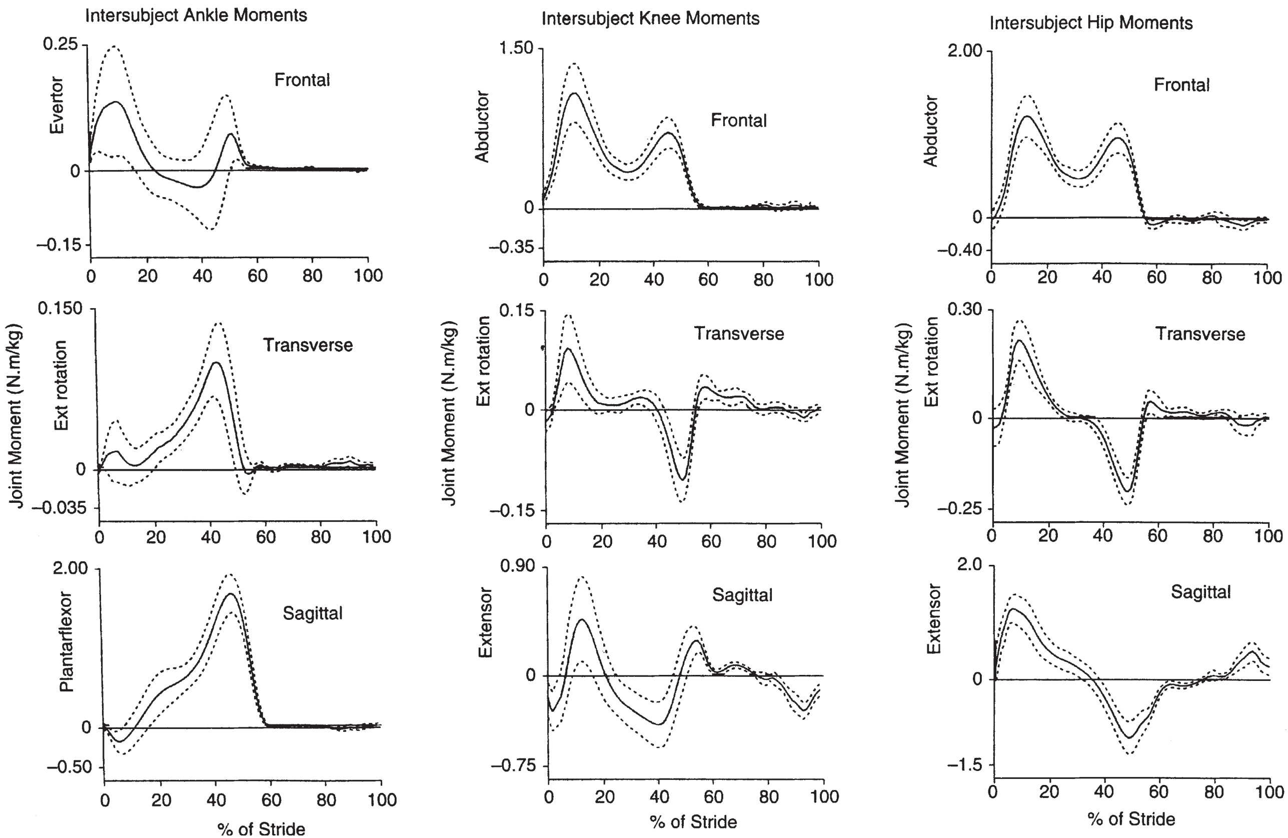

Figure 7.4 Typical 3D moments at the ankle, knee, and hip during one stride of walking (heel contact at 0 and 100%). Profiles are intersubject averages; solid line is the average curve with one standard deviation plotted as a dotted line. For interpretation of the more important profiles, see the text.

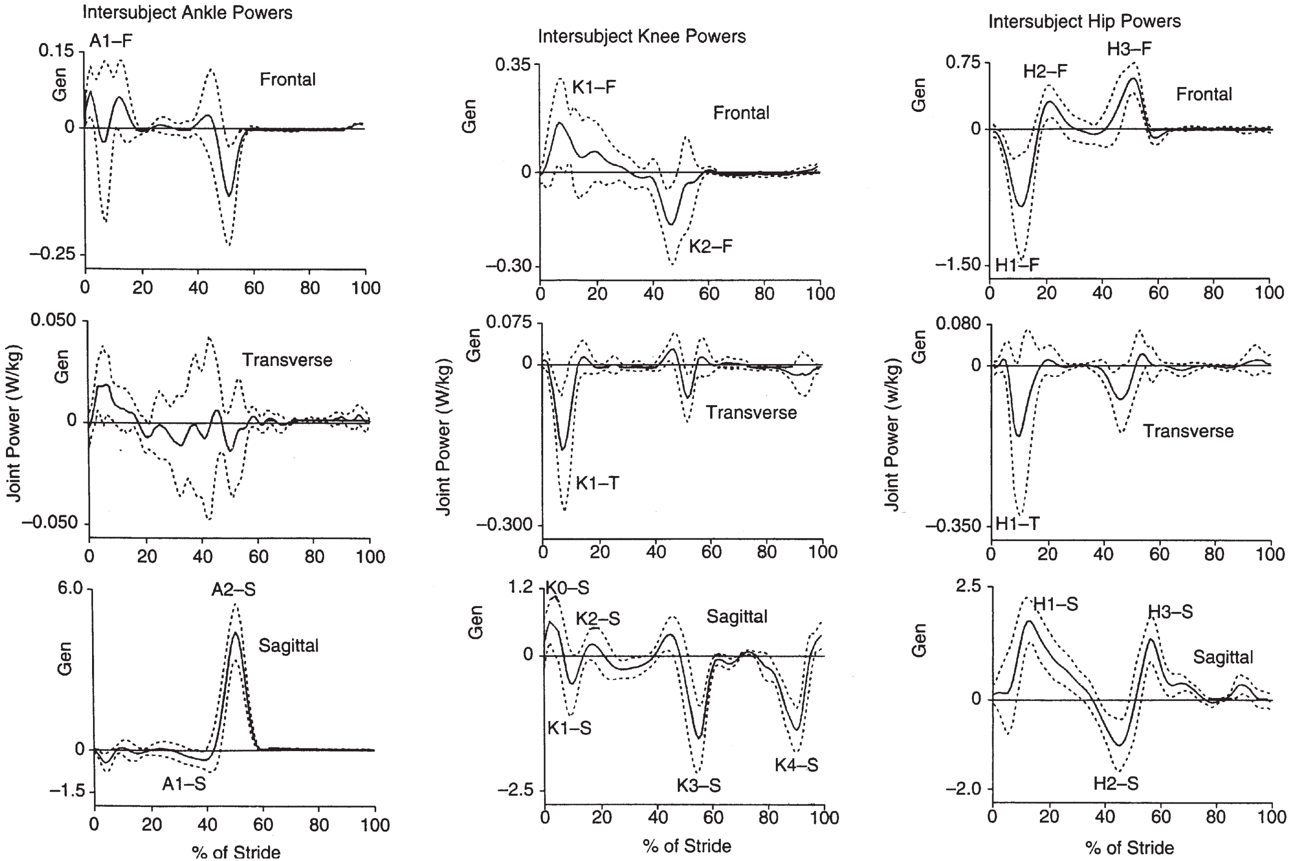

Figure 7.5 Mechanical power generation and absorption at the ankle, knee, and hip for the same averaged trials as in Figure 7.4. Generation power is $+ve$ and absorption power is $-ve$. For interpretation of selected profiles, see the text.

flexing forward under the influence of a large posterior reaction force at the hip; this also assists the knee extensors in preventing collapse of the knee joint and, in addition, contributes to forward propulsion by what has been described as a "push from behind" (H1-S generation burst). The flexor moment during the second half of stance serves two functions: first, to stabilize the trunk posture by preventing it from flexing backward under the influence of the forward reaction force at the hip; second, in the last phase of stance and early swing (50–75% of stride), to achieve a "pull-off" of the thigh into swing (H3-S generation burst).

4. The major transverse activity is at the hip. During the first half of stance, the external rotators of the stance limb act to decelerate the horizontal rotation of the pelvis (and trunk) over the stance limb (H1-T absorption phase); then, during the second half, the internal rotators are active to stabilize the forward rotation of the pelvis and swing limb.
5. The frontal plane moments at the stance hip are a strong abductor pattern to prevent drop of the pelvis (and entire upper body) against the forces of gravity, which are acting about 10 cm medial of the stance hip (H1-F absorption phase as the pelvis drops, followed by H2-F and H3-F generation phases as the pelvis, trunk, and swing limb are lifted to help achieve a safe toe clearance during swing). It is interesting to note a similar moment pattern at the stance knee, but this is not as a result of muscle activity. Rather, it is the response of the weight-bearing knee to the large gravitational load; the knee tries to invert but the passive loading of the medial condyles and unloading of the lateral condyles creates an internal abductor moment. Such an example illustrates the fact that internal skeletal and ligament structures can aid (or in some cases hinder) the activity of the muscles. Rehabilitation engineers involved in prothesis design must be aware of the internal moments created by the springs, dampers, and mechanical stops in their design.

7.5 SUGGESTED FURTHER READING

D'Sousa, A. F. and V. J. Garg. *Advanced Dynamics Modeling and Analysis* (Prentice-Hall, Englewood Cliffs, NJ, 1984).

Greenwood, D. T. *Principles of Dynamics*, *2nd edition*. (Prentice-Hall, Englewood Cliffs, NJ, 1988), Chapter 7.

Zatsiorsky, V. M. *Kinetics of Human Motion* (Human Kinetics, Champaign, IL, 2002).

7.6 REFERENCES

Davis, R. B., S. Õunpuu, D. Tyburski, and J. R. Gage. "A Gait Analysis Data Collection and Reduction Technique," *Human Movement Sci.* **10**:575–587, 1991.

Eng, J. J. and D. A. Winter. "Kinetic Analysis of the Lower Limbs during Walking: What Information Can Be Gained from a Three-dimensional Model," *J. Biomech*. **28**:753–758, 1995.

Õunpuu, S., R. B. Davis and P. A. DeLuca. "Joint Kinetics: Methods, Interpretation and Treatment Decision-Making in Children with Cerebral Palsy and Myelomeningocele," *Gait & Posture* **4**:62–78, 1996.